

Comparison between cold rotary forging and conventional forging[†]

Xinghui Han and Lin Hua^{*}

School of Materials Science and Engineering, Wuhan University of Technology, Wuhan, 430070, China

(Manuscript Received November 12, 2008; Received April 25, 2009, Accepted May 1, 2009)

Abstract

Cold rotary forging is an innovative incremental metal forming process, which is obviously different from the conventional forging process in many aspects, such as the metal flow, degree of inhomogeneous deformation of workpiece and force and power parameters. In the current work, a 3D elastic-plastic dynamic explicit FE model of cold rotary forging of a cylindrical workpiece is developed under the ABAQUS software environment and its validity has been verified by the experiment. Based on the reliable 3D FE model, the cold rotary forging and conventional forging processes are simulated and their difference in the forming process has been thoroughly clarified. The research results may help to understand the cold rotary forging process better. Furthermore, they provide valuable guidelines for further theoretical analysis and experimental studies on the cold rotary forging process.

Keywords: Cold rotary forging; Conventional forging; FE modeling; Deformation characteristics and mechanism

1. Introduction

With the development of industrial technology, precision forging, or net-shape forging, has become increasingly popular due to savings in material, energy and finishing steps. However, many of the new components, because of their shape complexity and complicated tool design and high load requirements, are challenging the current precision forging technology beyond its current level of technology. To meet the requirement, there is a renewed interest in incremental forming, especially rotary-type incremental forming processes, such as swaging, cross-wedge rolling, ring rolling, spinning and rotary forging.

Compared with the conventional forging technology, cold rotary forging offers the following advantages [1]: lower level of noise and vibration, uniform quality, smooth surface, close tolerance and considerable savings in energy and materials cost. Addition-

ally, because of the eccentric load in cold rotary forging, the stress state of cold rotary forging press is very complicated and the life of the bear is relatively low. At present, many studies have been done on the cold rotary forging process due to its significant advantages. In brief, these studies mainly focused on measuring the pressure distribution at the contact area [2], calculating and verifying the power parameters [3-6], and analyzing the metal flow [7-10] by using analytical and experimental methods. Meanwhile, the cold rotary forging process was analyzed by the rigid-plastic FE method [11-14]. All of these research results provided useful guidelines for further theoretical analysis and experimental studies on the cold rotary forging process. However, the deformation characteristics and mechanism of cold rotary forging at present have not been fully understood. Especially, the difference between cold rotary forging and conventional forging needs to be thoroughly clarified and studied further in order to better understand the cold rotary forging process. Because cold rotary forging is a very complex metal forming technology with multi-factors coupling interactive effects, it is difficult to obtain

[†]This paper was recommended for publication in revised form by Associate Editor Youngseog Lee

^{*}Corresponding author. Tel.: +86 27 8716 8391, Fax.: +86 27 8716 8391
E-mail address: lhuasvs@yahoo.com.cn

© KSME & Springer 2009

satisfactory results by analytical and experimental methods because of the limit of these methods. The finite element method has been proved a good method, which can obtain more detailed information in analyzing the metal forming processes. In cold rotary forging, the elastic deformation has a significant effect on the forming process and thus it is difficult to realize the acute simulation in the rigid-plastic FE analysis. Therefore, it is urgent to investigate the difference between cold rotary forging and conventional forging by the elastic-plastic FE method.

Consequently in this paper, the cold rotary forging and conventional forging process of a cylindrical workpiece is simulated by the elastic-plastic dynamic explicit FE method under the ABAQUS software environment. Through simulation, the deformation characteristics and mechanism of cold rotary forging are given and the difference between cold rotary forging and conventional forging is clarified in detail. The research results provide useful theoretical and experimental guidelines for the cold rotary forging process.

2. Establishment of 3D FE model of cold rotary forging

The principle of cold rotary forging is illustrated schematically in Fig.1. Different from conventional forging, the upper die in cold rotary forging is a conical die and can continuously oscillate around the vertical machine axis. Simultaneously the lower die pushes the workpiece continuously so as to cause the workpiece to be subjected to axial compression. Thus, when the workpiece is pressed repeatedly for several times, the plastic deformation of the workpiece will be completed perfectly.

From the above description, it can be seen that the deformation mechanism of cold rotary forging is very complex due to the periodical local loading and continuous shifting of the contact area. Therefore, it is necessary to investigate the cold rotary forging process by using FE method. Based on the forming characteristics, a 3D FE model of cold rotary forging of a cylindrical workpiece is developed under the ABAQUS software environment, as shown in Fig.2. The proposed 3D FE model has the following features.

(1) To improve the computation accuracy, the elastic-plastic FE method is adopted in the simulation.

- (2) In contrast to the static implicit procedure, the dynamic explicit procedure has unique advantages such as saving the solution costs and overcoming the convergence problem in simulating the complex contact and large deformation processes. Thus, the dynamic explicit procedure is used to simulate the cold rotary forging process which is a complex dynamic contact and highly non-linear metal forming technology.
- (3) The upper and lower die is defined as 3D analytical rigid body, while the cylindrical workpiece is defined as a 3D deformable solid body. The contact pairs are established between the dies and cylindrical workpiece. Meanwhile, the Coulomb friction model is used to describe the friction condition of the contact pairs due to the relative sliding existing between the dies and cylindrical workpiece.
- (4) The upper die is constrained to rotate only around the global 2-axis while the lower die is constrained to translate only along the global 2-axis. Because of the oscillation of the upper die, the cylindrical workpiece may rotate together with it and thus the cold rotary forging process cannot be performed successfully. Based on the deformation characteristics, the constraint type “distributing coupling” is adopted to constrain the rotation of the cylindrical workpiece.
- (5) In cold rotary forging, the contact surface between the upper die and workpiece is a portion of an Archimedes spiral surface. Thus, after the lower die stops the axial feed, the upper die still has to oscillate at least one revolution around the machine axis so as to make the upper surface of the cylindrical workpiece become a plane. To improve the surface quality of the upper surface of the cylindrical workpiece, the load curves of the upper and lower die are designed, as shown in Fig. 3.
- (6) The 3D linear reduction integration continuum element with eight nodes (C3D8R) is used to discretize the cylindrical workpiece. The number of the elements in the cylindrical workpiece is determined by its size and the computation efficiency and precision. Adaptive mesh technology is employed to reduce the distortion of elements.
- (7) Mass scaling technology is adopted in the simulation process. Appropriate mass scaling

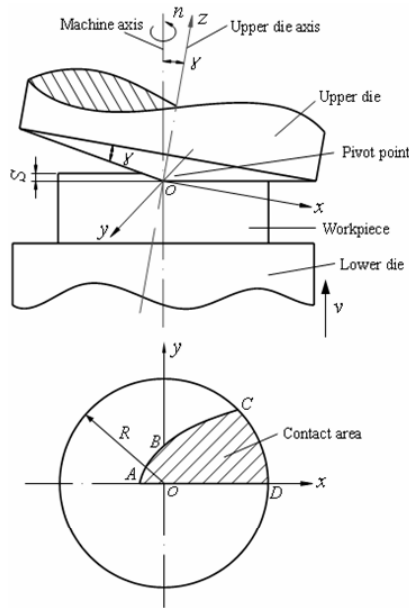


Fig. 1. Schematic diagram of cold rotary forging of the cylindrical workpiece.

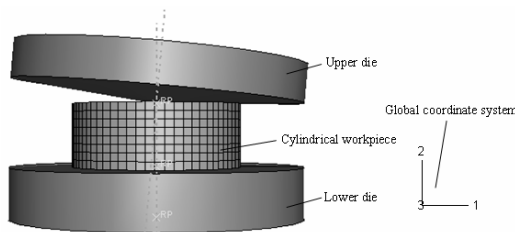


Fig. 2. 3D FE model of cold rotary forging of the cylindrical workpiece.

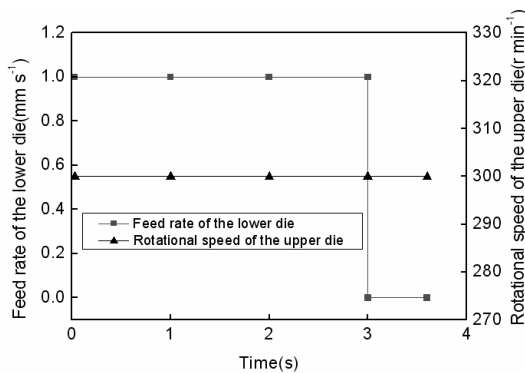


Fig. 3. Load curves of the upper and lower die in cold rotary forging.

factors are selected to improve the computation efficiency without sacrificing the computation accuracy.

Table 1. Processing parameters adopted in conventional forging.

Parameters	Values
Initial diameter of the cylindrical workpiece (mm)	40
Initial height of the cylindrical workpiece (mm)	15
Height reduction (%)	20
Feed rate of the upper die (mm s ⁻¹)	1
Friction coefficient between dies and workpiece	0.15

Table 2. Mechanical properties of the cylindrical workpiece.

Material	AISI1020
Density ρ (kg m ⁻³)	7800
Young's modulus E (GPa)	210
Poisson's ratio ν	0.3
Constitutive equation	$\sigma = 850\varepsilon^{0.25}$

Table 3. Processing parameters adopted in cold rotary forging.

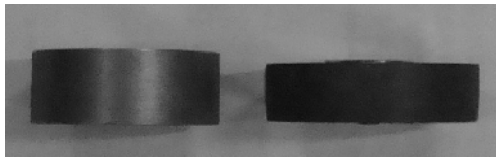
Parameters	Values
Initial diameter of the cylindrical workpiece (mm)	40
Initial height of the cylindrical workpiece (mm)	15
Height reduction (%)	20
Feed rate of the lower die (mm s ⁻¹)	1
Rotational speed of the upper die (r min ⁻¹)	300
Inclination angle of the upper die (°)	2
Friction coefficient between dies and workpiece	0.15
Motion orbit of the upper die	Circle line

3. Verification of the proposed 3D FE model of cold rotary forging

Conventional forging is a kind of basic metal forming process and its modeling technology has become very mature. Thus it is unnecessary to validate the 3D FE model of conventional forging. The processing parameters and the mechanical properties of the workpiece material adopted in conventional forging are shown in Table 1 and Table 2, respectively. The experiment of the cold rotary forging process is carried out on a T 200 cold rotary forging press at Hubei Automobile Axle Co., Ltd in China, as shown in Fig. 4. The press is hydraulically driven with the maximum capacity of 200 tons. Four types of motion orbit of the upper die have been available—circle, straight, spiral and rosette line on the T 200 cold rotary forging press. The circle line has been set for convenience of experimental control. The processing parameters adopted in cold rotary forging are shown in Table 3



Fig. 4. T 200 cold rotary forging press.



(a) Initial blank (b) Deformed cylindrical workpiece

Fig. 5. Initial blank and the deformed cylindrical workpiece.

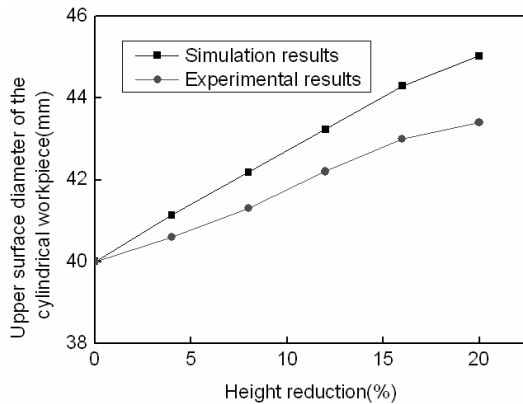
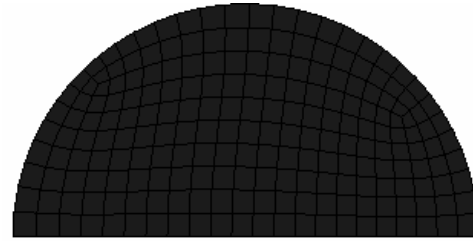
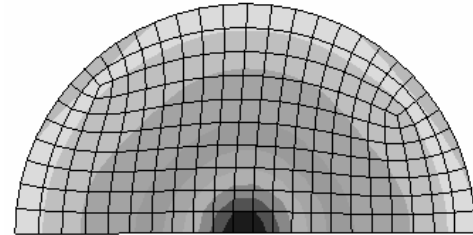


Fig. 6. Comparison between simulation results and experimental ones.

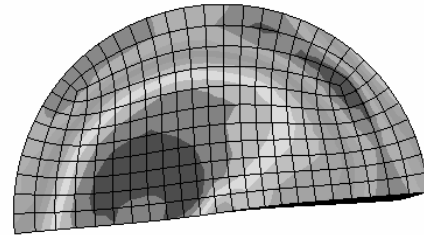
and the mechanical properties of workpiece material are shown in Table 2. MoS₂ is used as the lubricant in the experiment. The initial blank and the deformed cylindrical workpiece are shown in Fig. 5. Fig. 6 illustrates the comparison of the upper surface diameter of the cylindrical workpiece between the simulation



(a) Before deformation



(b) After deformation in conventional forging



(c) After deformation in cold rotary forging

Fig. 7. Comparison of mesh deformation between conventional forging and cold rotary forging.

and experimental results. It can be found from Fig.6 that the simulation results are in good agreement with the experimental ones and the maximum relative error is 3.76%. Thus, the 3D elastic-plastic dynamic explicit FE model of cold rotary forging of a cylindrical workpiece is proved to be reliable experimentally.

4. Results and discussion

4.1 Metal flow analysis

Fig. 7 shows the comparison of mesh deformation between conventional forging and cold rotary forging. It can be seen from Fig. 7(b) that in conventional forging, the metal only flows along two directions. One is the axial flow, resulting in thinning in the axial height of the cylindrical workpiece, and the other is the radial flow, leading to the expansion in diameter of the cylindrical workpiece. Obviously, metal flow does not exist in the circumferential direction. That is, because of the symmetry of geometry and boundary

conditions, the deformation of the cylindrical workpiece exhibits the characteristic of axial symmetrical deformation and thus conventional forging can be simplified as a 2D deformation process. In cold rotary forging, besides the axial and radial flow, the metal also flows along the circumferential direction, as shown in Fig.7 (c). Therefore, cold rotary forging is an asymmetrical deformation process and thereby the 3D analytical model has to be proposed to investigate the forming process.

4.2 Contact area between the dies and cylindrical workpiece

In conventional forging, the workpiece contacts with the upper and lower die completely at any time of the process. During the cold rotary forging process, the workpiece contacts the dies only partially because the upper die is a conical die. Furthermore, the contact area has been shifting continuously due to the oscillation of the upper die. Thus, the contact area exhibits a much complex and changeable geometry shape and thereby has an essential effect on the cold rotary forging process. Fig. 8 shows the contact area comparison between cold rotary forging and conventional forging. In conventional forging, the contact area between the upper die and workpiece is identical with that between the lower die and workpiece. It is clear that the contact area increases quasi-linearly from a certain value to the maximum value. Moreover, the curve is very smooth with time, indicating that the cylindrical workpiece is in a steady deformation state. Different from conventional forging, the contact area between the dies and workpiece in cold rotary forging is obviously different. The two curves can be divided into three different stages. At the beginning of cold rotary forging, the upper die begins to contact the workpiece, so the contact area between the upper die and workpiece increases rapidly from zero to a certain value while the contact area between the lower die and workpiece decreases significantly. As the forming process continues, the cylindrical workpiece has entered the steady deformation state; thus the contact area increases slowly up to the maximum value. At the end of the process, the lower die stops the axial feed while the upper die still oscillates, resulting in the sharp decrease in the contact area. Furthermore, it can be found that the two curves have been oscillating with time, indicating that cold rotary forging is a complex dynamic contact, highly nonlinear and non-

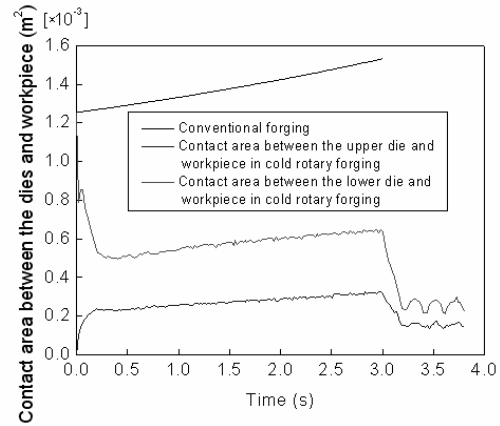


Fig. 8. Comparison of contact area between cold rotary forging and conventional forging.

steady-state deformation process. It can be also observed that the contact area between the upper die and workpiece is always smaller than that between the lower die and workpiece, thus leading to the higher axial unit pressure on the metal near the upper die. Under this circumstance, the metal near the upper die is easier to satisfy the yield condition to be involved in the plastic deformation state. From the above analysis, it can be concluded that the contact pattern, the shape and size of contact area between cold rotary forging and conventional forging are obviously different, thus resulting in the different deformation characteristics between them.

4.3 Plastic deformation zone (PDZ) distribution

In the metal plastic forming process, the shape and size of the PDZ has a significant effect on the forming process. Fig. 9 provides the PEEQ (equivalent plastic strain) distribution in the axial section of the cylindrical workpiece in conventional forging. It can be seen that the PDZ is formed firstly in the center part of the cylindrical workpiece, as shown in Fig. 9(b). As the process continues, the PDZ gradually develops toward the rest part and then the whole cylindrical workpiece becomes the PDZ at $t=0.615s$, as shown in Fig. 9(c). It can be also found from Fig. 9 that the center part of the cylindrical workpiece always has the maximum PEEQ value while the minimum PEEQ value always occurs in the middle part of the upper surface and the lower surface during the conventional forging process. The maximum and minimum PEEQ values are 0.2598 and 0.02165, respectively at the end

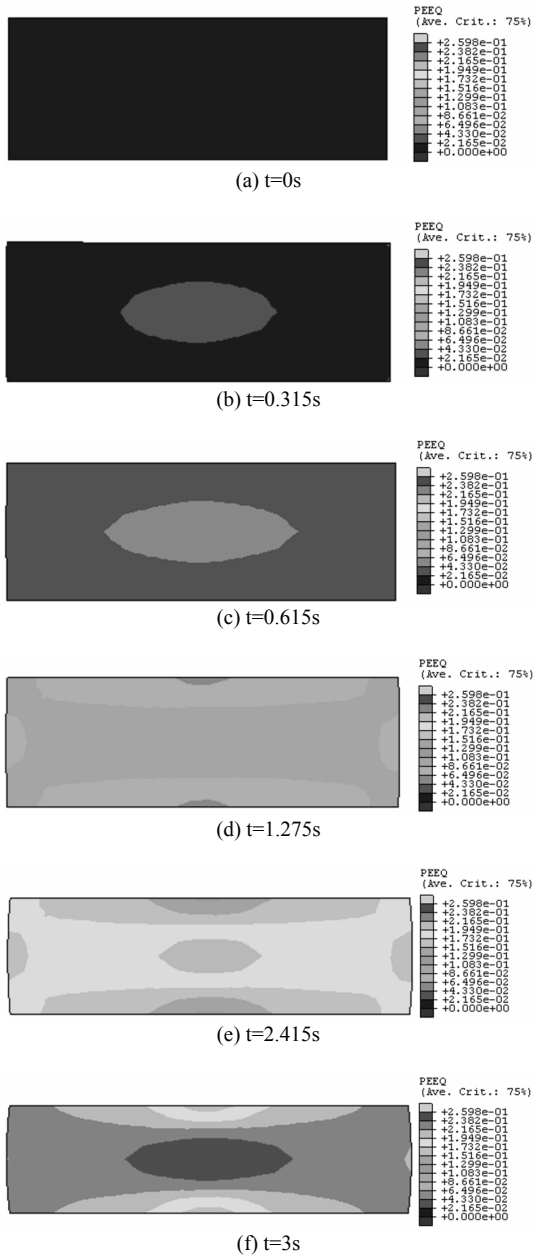


Fig. 9. PEEQ distribution in the axial section of the cylindrical workpiece in conventional forging.

of the process. If the difference between the maximum and minimum PEEQ is adopted to represent the degree of inhomogeneous deformation of the deformed cylindrical workpiece, the degree of inhomogeneous deformation in conventional forging is 0.23815. In addition, because of the symmetry of geometry and boundary conditions, the PDZ distribu-

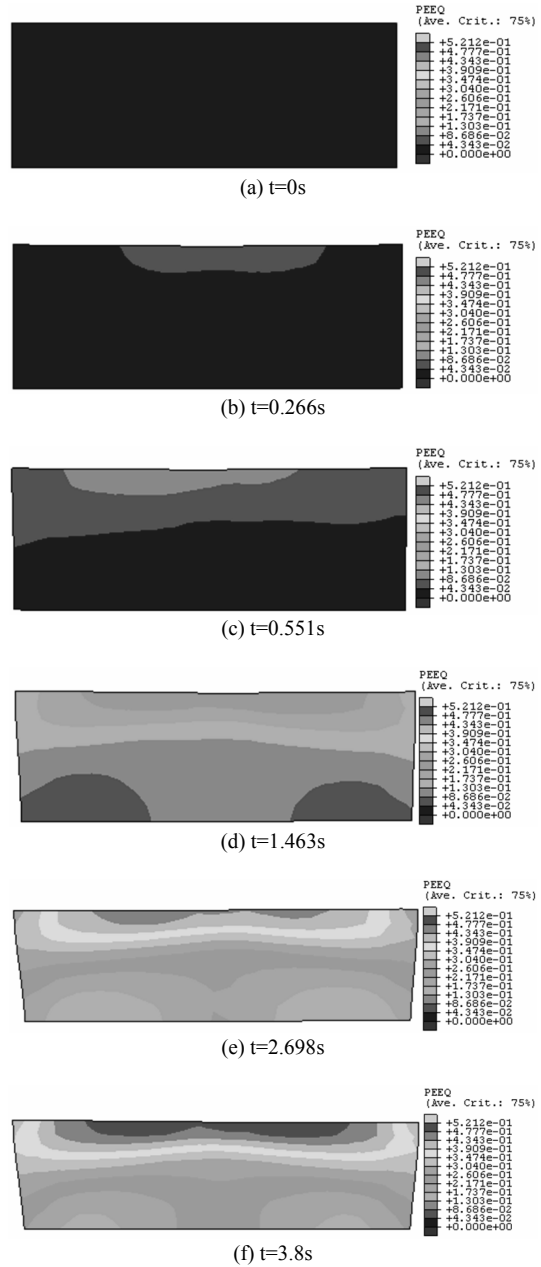


Fig. 10. PEEQ distribution in the axial section of the cylindrical workpiece in cold rotary forging.

tion in conventional forging exhibits the symmetry in the axial and radial direction.

Fig. 10 shows the PEEQ distribution in the axial section of the cylindrical workpiece in cold rotary forging. As described above, the upper region of the cylindrical workpiece is easier to satisfy the yield condition to come into the plastic deformation state.

So at the beginning of the process, the middle part of the upper surface firstly produces the plastic deformation, as shown in Fig. 10(b). Under the action of the axial feed of the lower die and the oscillation of the upper die, the PDZ gradually expands radially toward the cylindrical surface and axially toward the lower surface, as shown in Fig. 10(c). At $t=1.463s$, the PDZ penetrates the axial height and the whole cylindrical workpiece is involved in the plastic deformation, as shown in Fig. 10(d). It can be also observed from Fig. 10 that just like a kind of wave, the PEEQ exhibits a transfer characteristic from the upper surface to the lower surface of the cylindrical workpiece. During the whole cold rotary forging process, the maximum PEEQ value occurs in the middle part of the upper surface while the metal located in the lower surface has the minimum PEEQ value at any time of the process. At the end of the process, the maximum and minimum PEEQ values are 0.5212 and 0.04343, respectively. The degree of inhomogeneous deformation of the cylindrical workpiece is 0.47777. Different from conventional forging, the PEEQ distribution in cold rotary forging is only approximately symmetrical in the radial direction while it is asymmetrical in the axial direction because of the asymmetrical boundary conditions.

To reveal the PEEQ distribution law in detail, some special points in the axial section of the cylindrical workpiece are selected as the tracking points for measuring the PEEQ values, as shown in Fig. 11. All the tracking points are located in the half of the axial section owing to the PEEQ distribution symmetry in the radial direction. Fig. 12 illustrates the comparison of PEEQ distribution of tracking points along the radial direction between cold rotary forging and conventional forging. It can be observed from Fig. 12(a) that in conventional forging, the PEEQ value along A-B line and E-F line is identical, which coincides with the PEEQ distribution symmetry in the axial direction. Furthermore, the PEEQ value gradually decreases along C-D line, while it gradually increases along A-B and E-F line. By comparing the three curves, it can be also concluded that the PEEQ value of the middle part is larger than that of the upper and lower region of the cylindrical workpiece. In cold rotary forging, the PEEQ value gradually decreases from A-B line to E-F line (shown in Fig. 12(b)), which also coincides with the PEEQ transfer characteristic from the upper surface to the lower surface of the cylindrical workpiece.

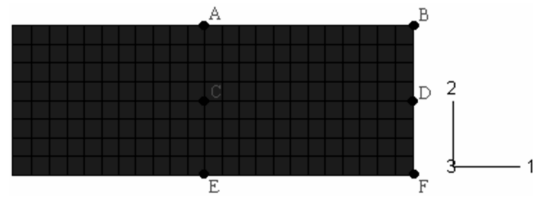
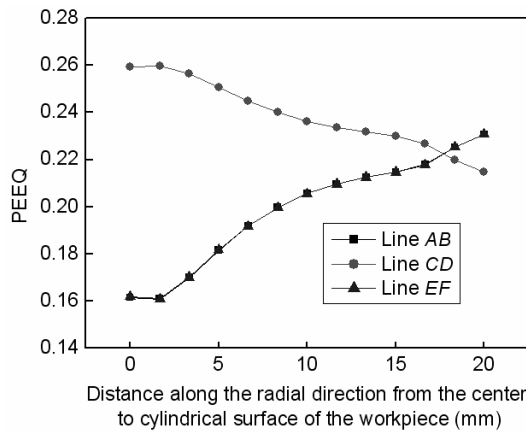


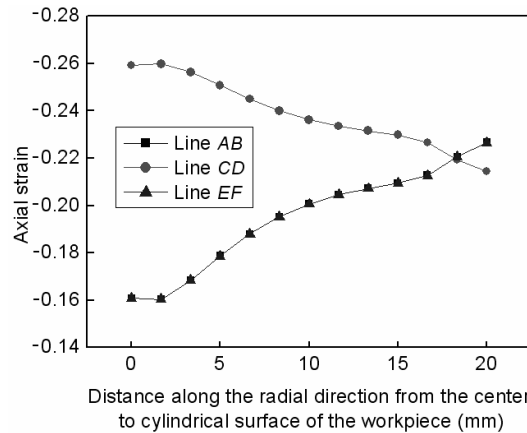
Fig. 11. Tracking points in the axial section of the cylindrical workpiece.

Fig. 13 describes the strain components (axial, circumferential and radial strain) distribution of tracking points along the radial direction in conventional forging. It can be seen from Fig. 13 that just as the PEEQ distribution, the strain components of the middle part are larger than that of the upper and lower region of the cylindrical workpiece. The strain components distribution of tracking points along the radial direction in cold rotary forging is shown in Fig. 14. From Fig. 14, it can be found that all the strain components gradually decrease from the upper surface to the lower surface of the cylindrical workpiece.

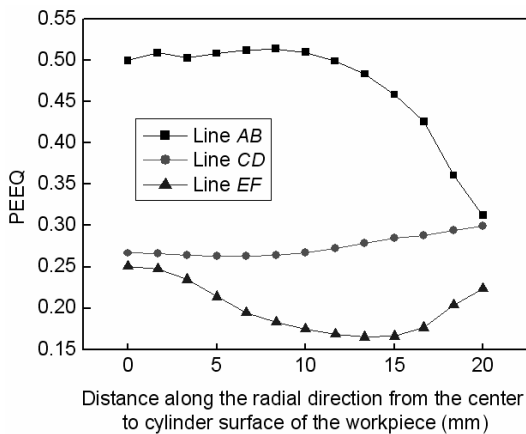
From the above analysis, it can be concluded that in conventional forging, the metal of the upper and lower region of the cylindrical workpiece is relatively hard to flow because of the friction force. So the strains including PEEQ and strain components of the upper and lower region are relatively smaller. Inversely, the metal of the middle part is easy to flow because the effect of friction is smaller, thus resulting in the larger strains of the middle part of the cylindrical workpiece. Under this circumstance, the cylindrical workpiece exhibits the “drum” effect (shown in Fig. 9), which is the main characteristic of conventional forging. In cold rotary forging, the strains including PEEQ and strain components gradually decrease from the upper surface to the lower surface. So the “mushroom” effect of the deforming cylindrical workpiece occurs (shown in Fig. 10), which is the main characteristic of cold rotary forging. In the production of some parts such as the half-shaft used in the automobile and the coupler knuckle pin (a flange with a long rod), the mushroom effect can be used to form the head. The mushroom effect also has a wide application in the riveting process. When the mushroom effect is obvious, the rod of the rivet is in elastic or small plastic deformation state so as to achieve the loose riveting. Inversely, when the mushroom effect is not so obvious, the rod of the rivet is in large plastic deformation state so as to achieve the tight riveting.



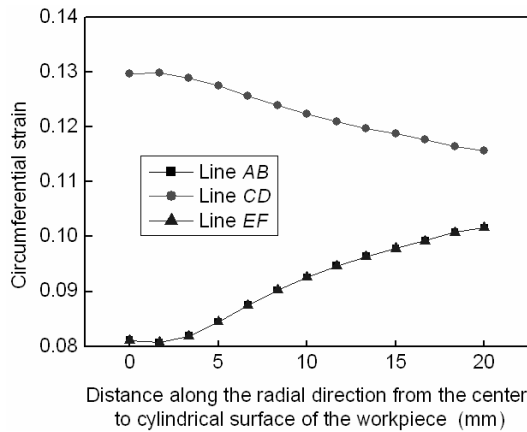
(a) PEEQ distribution of tracking points along the radial direction in conventional forging



(a) Axial strain distribution of tracking points along the radial direction



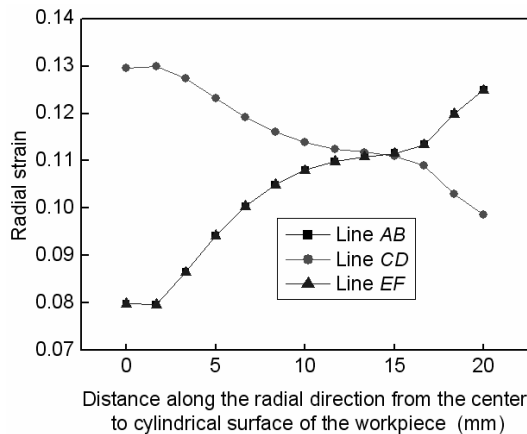
(b) PEEQ distribution of tracking points along the radial direction in cold rotary forging



(b) Circumferential strain distribution of tracking points along the radial direction

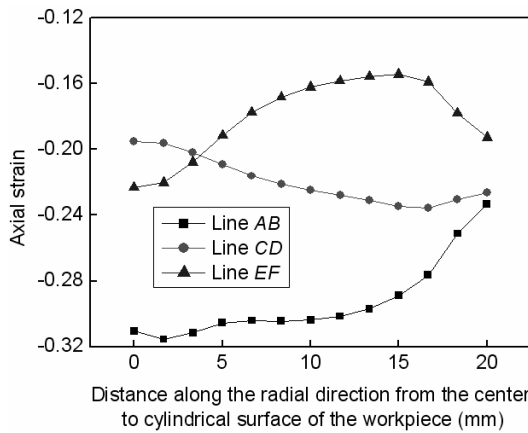
Fig. 12. Comparison of PEEQ distribution of tracking points along the radial direction between cold rotary forging and conventional forging.

Fig. 15 represents the comparison of PEEQ history of tracking points between conventional forging and cold rotary forging. In conventional forging, the strains of tracking points gradually increase quasi-linearly with time, as shown in Fig. 15(a). In cold rotary forging (shown in Fig. 15(b)), the strain of every tracking point increases stepwise, which is caused by the continuous shifting of the plastic deformation zone. It is obvious that each step represents one revolution of the upper die. When the upper die contacts the cylindrical workpiece, the strains of tracking points located in the contact area increase rapidly. That is, the height of the step represents the strains of tracking points in a single revolution. The level part of the step corresponds to the time when the

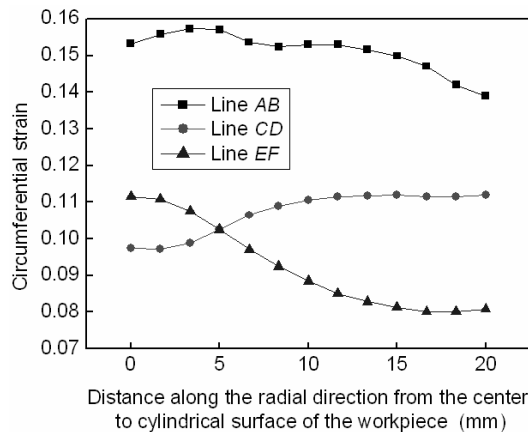


(c) Radial strain distribution of tracking points along the radial direction

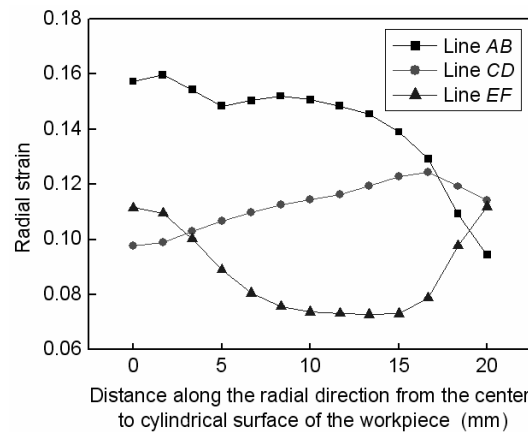
Fig. 13. Strain components distribution of tracking points along the radial direction in conventional forging.



(a) Axial strain distribution of tracking points along the radial direction

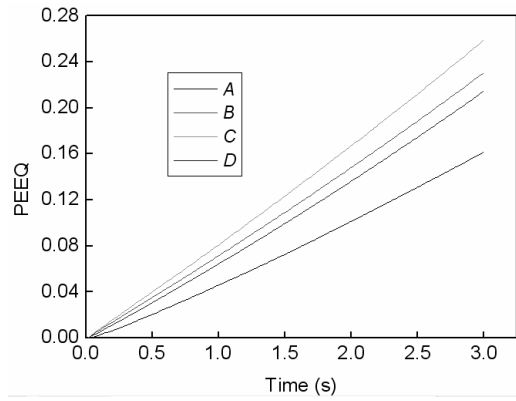


(b) Circumferential strain distribution of tracking points along the radial direction

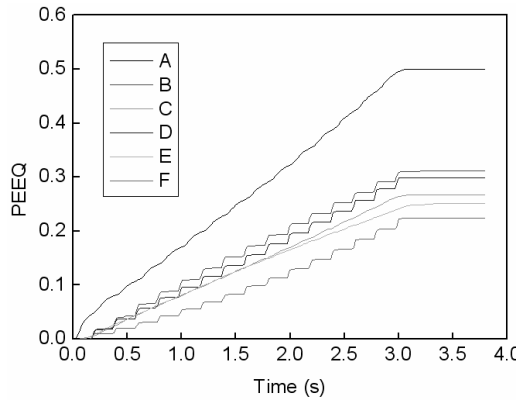


(c) Radial strain distribution of tracking points along the radial direction

Fig. 14. Strain components distribution of tracking points along the radial direction in cold rotary forging.



(a) PEEQ history of tracking points in conventional forging



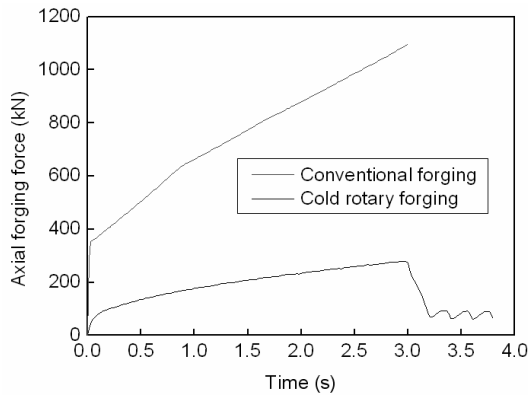
(b) PEEQ history of tracking points in cold rotary forging

Fig. 15. Comparison of PEEQ history of tracking points between conventional forging and cold rotary forging.

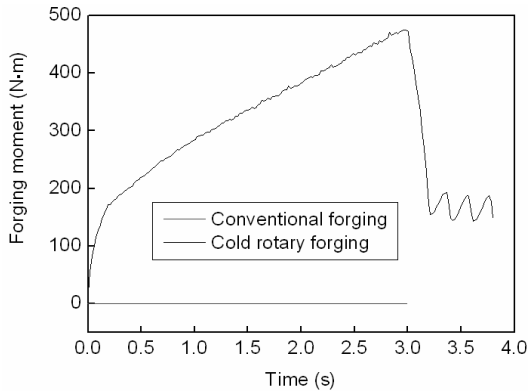
upper die deviates from the contact area. After 3s of the cold rotary forging process, the lower die stops the axial feed while the upper die still oscillates, and the strains of all the tracking points increase no longer with time. Therefore, these values of strains are the strains of the final cold rotary forging products. Based on the above analysis, it can be concluded that conventional forging is an overall plastic forming process in which the strains gradually increase quasi-linearly with time. In cold rotary forging, the desired total strains are achieved by a large number of small steps and cold rotary forging can thus be described as an incremental metal forming process.

4.4 Force and power parameters

Fig. 16 provides a comparison of force and power parameters between conventional forging and cold rotary forging. From Fig. 16(a), it can be seen that the variation curve of axial forging force is composed of



(a) Comparison of axial forging force between conventional forging and cold rotary forging



(b) Comparison of forging moment between conventional forging and cold rotary forging

Fig. 16. Comparison of force and power parameters between conventional forging and cold rotary forging.

two different stages in the conventional forging process. At the beginning of the process, the axial forging force increases significantly from zero to a certain value. And then it gradually increases quasi-linearly. It is also observed from Fig. 16(b) that the forging moment is zero during the whole conventional forging process. From Fig. 16, also, the cold rotary forging process has experienced three deformation stages. At the first stage, the upper die begins to contact the cylindrical workpiece and thus the axial forging force and forging moment increase rapidly from zero to a certain value. At the second stage, the axial forging force and forging moment increase slowly up to the maximum value, indicating that the cylindrical workpiece has entered the steady deformation stage. At the last one, the lower die stops the axial feed while the upper die still oscillates, thus resulting in less metal to participate in the plastic deformation. So the axial

forging force and forging moment decrease sharply. In conventional forging, the maximum axial forging force is 1095.66 kN, while the maximum axial forging force and forging moment in cold rotary forging are 280.3 kN and 475.23 N·m, respectively. It shows that the maximum axial forging force of conventional forging is fourth time of that of cold rotary forging. From the above analysis it can be found that as a kind of incremental metal forming process, cold rotary forging can reduce the forging force significantly.

5. Conclusions

A 3D elastic-plastic dynamic explicit FE model of cold rotary forging of a cylindrical workpiece is developed under the ABAQUS software environment and its validity has been verified by the experiment. Based on the reliable 3D FE model, the difference between cold rotary forging and conventional forging has been thoroughly clarified. The research results show the following.

- (1) Conventional forging exhibits the characteristic of axial symmetrical deformation and thus it can be simplified as a 2D deformation process. Whereas, cold rotary forging is an asymmetrical deformation process, and thereby a 3D analytical model has to be proposed to investigate the forming process.
- (2) Conventional forging is an overall plastic forming process in which the strains gradually increase quasi-linearly with time. Whereas, cold rotary forging is a process of strain accumulation by a large number of small strain steps and thus it is considered to be an incremental forming technology.
- (3) In conventional forging, the middle part of the cylindrical workpiece has the larger strains (PEEQ and strain components) than the upper and lower region. So the deformed cylindrical workpiece exhibits the drum effect. In cold rotary forging, the strains (PEEQ and strain components) gradually decrease from the upper surface to the lower surface, thus resulting in the obvious mushroom effect of the deformed cylindrical workpiece.
- (4) The workpiece-upper die contact area in cold rotary forging is much smaller than the one observed in conventional forging, so the force and power necessary to deform are reduced to a small fraction of that of conventional forging

technologies.

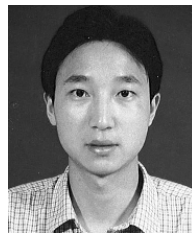
- (5) The research results thoroughly clarify the difference between cold rotary forging and conventional forging, and provide useful theoretical and experimental guidelines for the cold rotary forging process.

Acknowledgment

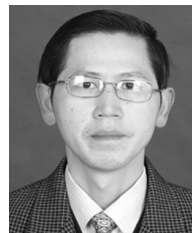
The authors would like to thank the Natural Science Foundation of China for Distinguished Young Scholars (No. 50725517) for the support given to this research.

References

- [1] X. H. Pei, M. Zhang and Y. M. Hu, *Rotary Forging*, Mechanical Industry Press, Beijing, China, (1991).
- [2] J. B. Hawkyard, C. K. S. Gurnani and W. Johnson, Pressure-distribution measurements in rotary forging, *J. Mech. Eng. Sci.* 19 (4) (1977) 135-142.
- [3] M. Zhang, Calculating force and energy during rotary forging, *Proc. of the 3rd International Conference on Rotary Metalworking Processes*, Kyoto, Japan (1984) 115-124.
- [4] J. Oudin, Y. Ravalard, G. Verwaerde and J. C. Gelin, Force, torque and plastic flow analysis in rotary upsetting of ring shaped billets, *Int. J. Mech. Sci.* 27 (11-12) (1985) 761-780.
- [5] S. Choi, K. H. Na and J. H. Kim, Upper-bound analysis of the rotary forging of a cylindrical billet, *J. Mater. Process. Technol.* 67 (1-3) (1997) 78-82.
- [6] T. Canta, D. Frunza, D. Sabadus and C. Tintelecan, Some aspects of energy distribution in rotary forming processes, *J. Mater. Process. Technol.* 80-81 (1998) 195-198.
- [7] P. M. Standring, J. R. Moon and E. Appleton, Plastic deformation produced during indentation phase of rotary forging, *Met. Technol.* 7 (3) (1980) 159-166.
- [8] D. C. Zhou, Y. D. Han and Z. R. Wang, Research on rotary forging and its distribution of deformation, *J. Mater. Process. Technol.* 31 (1-2) (1992) 161-168.
- [9] H. K. Oh and S. Choi, A study on center thinning in the rotary forging of a circular plate, *J. Mater. Process. Technol.* 66 (1-3) (1997) 101-106.
- [10] G. C. Wang, J. Guan and G. Q. Zhao, A photo-plastic experimental study on deformation of rotary forging a ring workpiece, *J. Mater. Process. Technol.* 169 (1) (2005) 108-114.
- [11] S. J. Yuan, X. H. Wang, G. Liu and D. C. Zhou, The precision forming of pin parts by cold-drawing and rotary-forging, *J. Mater. Process. Technol.* 86 (1-3) (1998) 252-256.
- [12] G. C. Wang and G. Q. Zhao, A three-dimensional rigid-plastic FEM analysis of rotary forging deformation of a ring workpiece, *J. Mater. Process. Technol.* 95 (1-3) (1999) 112-115.
- [13] G. C. Wang and G. Q. Zhao, Simulation and analysis of rotary forging a ring workpiece using finite element method, *Finite. Elem. Anal. Des.* 38 (12) (2002) 1151-1164.
- [14] G. Liu, S. J. Yuan, Z. R. Wang and D. C. Zhou, Explanation of the mushroom effect in the rotary forging of a cylinder, *J. Mater. Process. Technol.* 151 (1-3) (2004) 178-182.



Xinghui Han received his M.S. degree in Materials Processing Engineering from Wuhan University of Technology, China, in 2007. He is currently a Ph. D. candidate at the School of Materials Science and Engineering at Wuhan University of Technology in Wuhan, China. Dr. Han's research interests include advanced forming and equipment technology.



Lin Hua received his M.S. degree in Pressure Processing from Wuhan University of Technology, China, in 1985. He then received his Ph.D. degree in Mechanical Engineering from Xi'an Jiaotong University, China, in 2000. Dr. Hua is currently a professor at the School of Materials Science and Engineering at Wuhan University of Technology in Wuhan, China. Dr. Hua's research interests include advanced forming and equipment technology.